Supplement of

Water enhances the formation of fragmentation products via the cross-reactions of RO_2 and HO_2 in the photooxidation of isoprene

Jiayun Xu et al.

Correspondence to: Zhongming Chen (zmchen@pku.edu.cn)

Calculation of OH exposure (OH_{exp})

OH_{exp} equals the product of OH concentration and exposure time of reactants in the reaction system. It serves as a characterization of the oxidation process by OH radical. We used the decay of isoprene to calculate OH_{exp} under different exposure times before its concentration decreased below the detection limit (Eq. (S1)) (Lambe et al., 2011). The concentrations of MACR and MVK reached the peak almost at the same time when the concentration of isoprene fell below the detection limit. We define the measured peak concentrations of MACR and MVK as $[MACR]_{t0}$ and $[MVK]_{t0}$. When the concentration of isoprene was too low to be detected (<5 ppbv), an additional OH_{exp} ($OH_{exp,add}$, Eq. (S2)) determined from MACR and MVK decay was added to OH_{exp}. The calculation results of OH_{exp} in Exp. 1−4 were shown in Fig. S1. The uncertainty of OH_{exp} is within ± 15 %.

$$OH_{exp} = \frac{1}{k_{OH,ISO}} \times -ln\frac{[ISO]_t}{[ISO]_0} \quad \text{(S1)}$$

$$OH_{exp,add} = \frac{1}{2} \times \frac{1}{k_{OH,ISO}} \times \left(-ln\frac{[MACR]_t}{[MACR]_{t0}} + -ln\frac{[MVK]_t}{[MVK]_{t0}}\right) \quad \text{(S2)}$$

Calculation of atmospheric equivalent photochemical age (atmospheric EPA)

Atmospheric EPA refers to the equivalent time scale of photooxidation in a certain experiment to that in the ambient atmosphere, generally in a unit of hours or days. It can be calculated with Eq. (S3). Here we used the average OH concentration in the troposphere measured by Mao et al. (2009), 1.5×10^6 molec cm^{-3}, as a surrogate for atmospheric OH concentration ($[OH]$).

$$Atmospheric\ EPA\ (hrs) = \frac{OH_{exp}}{[OH] \times 3600} \quad \text{(S3)}$$

Corrections for products molar yields

We made a series of corrections to eliminate the effect of secondary OH oxidation, photolysis, and wall loss of concerning products on the determination of their actual yields. The correction for secondary OH oxidation was achieved by multiplying the correction factor $F_{1\,PRO,i}(t)$ (Eq. (S5)) (Ruppert and Heinz Becker, 2000) to the observed molar yields $Y_{PRO,i}(t)$ (Eq. (S4)). A second correction factor, $F_{2\,PRO,i}(t)$ (Eq. (S7)), derived from pseudo first-order reaction kinetic equation was applied to correct wall loss and photolysis loss. First-order wall loss and photolysis rate constants ($k_{WALL,i}$ and $k_{PH,i}$) and second-order OH reaction rate constants ($k_{PRO,i+OH}$) for the concerned products in our experiments were listed in Table S2, S3 and S4.

$$Y_{PRO,i}(t) = \frac{\Delta M_{PRO,i}(t)}{\Delta M_{ISO}(t)} \quad \text{(S4)}$$

$$F_{1\ PRO,i}(t) = \left(\frac{k_{ISO+OH} - k_{PRO,i+OH}}{k_{ISO+OH}}\right)\left(\frac{1-C_t}{C_t^{\,k_{PRO,i+OH}/k_{ISO+OH}} - C_t}\right) \quad \text{(S5)}$$

$$C_t = [ISO]_t/[ISO]_0 \quad \text{(S6)}$$

$$F_{2\ PRO,i}(t) = e^{-k_{WALL,i}\times t - k_{PH,i}\times t} \quad \text{(S7)}$$

$$Y'_{PRO,i}(t) = Y_{PRO,i}(t) \times F_{1\ PRO,i}(t)/F_{2\ PRO,i}(t) \quad \text{(S8)}$$

Determination of OH and HO_2 concentrations

OH, and HO_2 concentrations are basic inputs in model simulations. In the present study, the photooxidation process in the OFR was divided into six sampling periods (0−10 s, 11−20 s, 21−30 s, 31−40 s, 41−50 s, 51−61 s). The average OH concentration in each sampling period was obtained by dividing the increment of OH_{exp} and residence time in this period. HO_2 was constrained by H_2O_2 concentrations measured in the experiments (see Fig. S3). Eq. (S9), derived from the mass balance for production and loss of H_2O_2, was used to calculate HO_2 concentration in individual sampling periods. The dominant production pathways for H_2O_2 in the experiments were self-combination of OH and disproportionation of HO_2, while the major loss pathway was its reaction with OH. $P_{H_2O_2}$, $[OH]$ and $[H_2O_2]$ in Eq. (S9) refers to the average value of H_2O_2 production rate, OH concentration, and H_2O_2 concentration in each sampling period. The related reaction rate constants are available in Atkinson et al. (2004).

$$[HO_2] = \sqrt{\frac{P_{H_2O_2} - k_{OH+OH}\,[OH]^2 + k_{OH+H_2O_2}\,[OH][H_2O_2]}{k_{HO_2+HO_2}}} \quad \text{(S9)}$$

Distribution of RO_2 reaction pathways

We calculated the distribution of RO_2 reaction pathways in the experiments under four conditions based on the reaction rates of HO_2, RO_2, and H-shift pathways (units: s^{-1}) following the method in Liu et al. (2013). Total RO_2 concentrations in the four experiments were simulated employing a box model. The determination of HO_2 concentrations has been described above. For Exp.1 and 2 representing first-generation reactions, RO_2 here refers to β-1,2-ISOPOO and β-4,3-ISOPOO. The reaction rate constants for HO_2, RO_2, and H-shift pathways are the weighted mean values for the two isomers. For Exp. 3 and 4 representing multi-generation reactions, RO_2 refers to the assembling of a series of RO_2 the sum of whose concentrations takes more than 90 % of the total concentration of RO_2 (specifically, ISOPBO2, ISOPDO2,

C59O2, CH3O2, C57O2, C58AO2, HMVKBO2 and CHOMOHCO3, the names of the above-mentioned RO_2 are consistent with those in MCM v3.3.1). The results are presented in Fig. S2.

Parameterization of the water effect on reaction rate constants

Previous studies have pointed out that water vapor can accelerate the self-reactions of RO_2 via the formation of water complexes ($RO_2 \cdot H_2O$) (Clark et al., 2008; Clark et al., 2010; Kumbhani et al., 2015). We assume this water effect also exists in the HO_2 reactions with RO_2 in that HO_2 can complex with H_2O as well (Kircher and Sander, 1984). Here we referred to an experimental study based on β-hydroxy ethyl peroxy (β-HEP), whose structure and binding energy with H_2O are similar to that of β-ISOPOO, to parameterize this water effect on the RO_2 and HO_2 reactions with β-ISOPOO isomers (Kumbhani et al., 2015). An additional term $k'_{RO_2(HO_2)}$ (Eq. (S10)) was added to their rate constants in MCM v3.3.1. $R_{RO_2\,(HO_2)\,\cdot\,H_2O}$ and $R_{\beta-HEP\,\cdot\,H_2O}$ refers to the relative abundance of RO_2- (or HO_2-) water complexes and β-HEP-water complexes, separately, and their values are available in Table S5. The term $(13.2 \times 10^{-44}\, e^{9538\,/\,T} \times [H_2O])$ represents the temperature- and water-dependent calibration for the self-reaction rate constant of β-HEP derived from Kumbhani et al. (2015). For the HO_2 reaction with β-ISOPOO isomers, $R_{RO_2\,(HO_2)\,\cdot\,H_2O}$ in Eq. S10 was replaced by the geometric average of the relative abundance of $HO_2 \cdot H_2O$ and β-ISOPOO$\cdot H_2O$ ($\sqrt{R_{HO_2\cdot H_2O}\, R_{\beta-ISOPOO\cdot H_2O}}$). Same reaction rate constants were given to β-ISOPOO permutation reactions with all related RO_2 species in isoprene photooxidation for simplification.

$$k'_{RO_2(HO_2)} = \frac{R_{RO_2\,(HO_2)\,\cdot\,H_2O}}{R_{\beta-HEP\,\cdot\,H_2O}} \times (13.2 \times 10^{-44}\, e^{9538\,/\,T} \times [H_2O]) \qquad \text{(S10)}$$

Chemicals

The following chemicals were used to prepare standard solutions for instrument calibration without purification: hydrogen peroxide (H_2O_2; Alfa Aesar, 35 wt. %), formaldehyde (HCHO; Sigma-Aldrich, 37 wt. %), glyoxal (GLY; Sigma-Aldrich, 40 wt. %), methylglyoxal (MGLY; Sigma-Aldrich, 40 wt. %), hydroxy acetone (HACE; Sigma-Aldrich, 90 %), methacrolein (MACR; Sigma-Aldrich, 96 %), formic acid (FA; Sigma-Aldrich, 98 %), acetic acid (AA; Sigma-Aldrich, 99.7 %).

Other chemicals used in the experiments: ammonia solution and ammonium chloride ($NH_3 \cdot H_2O$ and NH_4Cl, Beijing Tongguang Fine Chemicals Company, 25.0−28.0 % and ≥ 99.5 %), potassium iodide (KI;

Aladdin Chemical Inc., Shanghai, China, 99.99 %), orthophosphoric acid (H_3PO_4; Fluka, 85−90 %), hemin (Sigma-Aldrich, ≥ 98.0 %), 4-hydroxyphenyl acetic acid (Alfa Aesar, 99 %). They were used without purification as well.

Figure captions.

Figure S1. The evolution of OH_{exp} with residence time in Exp. 1−4 (a−d).

Figure S2. Distribution of reaction pathways of major RO_2 in the experiments. Major RO_2 refers to RO_2 species which consist of more than 90 % of total RO_2 concentrations. In (a) Exp. 1 and (b) Exp. 2 it refers to β-ISOPOO, while in (c) Exp. 3 and (d) Exp. 4 refers to the assembly of a series of RO_2.

Figure S3. The observed evolution of H_2O_2 concentration in the experiments. Corrections have been made to eliminate photolysis and wall loss of H_2O_2. The error bars represent ± standard deviation (± SD) based on 6 measurements.

Table captions.

Table S1. Collection efficiencies for different species by the rinsing solution (5×10^{-3} M H_3PO_4 or ultrapure water) in the coiling tube at 277 K.

Table S2. First-order wall loss rate constants ($k_{WALL,i}$) of the concerned products in the OFR.

Table S3. First-order photolysis rate constants ($k_{PH,i}$) of the concerned products in the OFR.

Table S4. Second-order reaction rate constants of the concerned products with OH radicals at 298 K ($k_{PRO,i+OH}$). The reaction rate constants were abstracted from MCM v3.3.1 website (http://mcm.york.ac.uk/home.htt) except for that of HMHP and β-ISOPOOH, which were abstracted from Allen et al. (2018) and St Clair et al. (2016), separately.

Table S5. Relative abundance of RO_2 (HO_2) water complexes ($R_{RO_2\ (HO_2)\cdot H_2O}$) at 298 K under 30 % and 80 % RH.

Table S6. Advanced mechanisms and kinetics of isoprene photooxidation to MCM v3.3.1 in the modeling in this study.

References

Allen, H. M., Crounse, J. D., Bates, K. H., Teng, A. P., Krawiec-Thayer, M. P., Rivera-Rios, J. C., Keutsch, F. N., St Clair, J. M., Hanisco, T. F., Moller, K. H., Kjaergaard, H. G. and Wennberg, P. O.: Kinetics and product yields of the OH initiated oxidation of hydroxymethyl hydroperoxide, J. Phys. Chem. A, 122, 6292-6302, doi: 10.1021/acs.jpca.8b04577, 2018.

Atkinson, R., Baulch, D. L., Cox, R. A., Crowley, J. N., Hampson, R. F., Hynes, R. G., Jenkin, M. E., Rossi, M. J. and Troe, J.: Evaluated kinetic and photochemical data for atmospheric chemistry: Volume I - gas phase reactions of O_x, HO_x, NO_x and SO_x species, Atmos. Chem. Phys., 4, 1461-1738, doi: 10.5194/acp-4-1461-2004, 2004.

Atkinson, R., Baulch, D. L., Cox, R. A., Crowley, J. N., Hampson, R. F., Hynes, R. G., Jenkin, M. E., Rossi, M. J., Troe, J. and Subcommittee, I.: Evaluated kinetic and photochemical data for atmospheric chemistry: Volume II - gas phase reactions of organic species, Atmos. Chem. Phys., 6, 3625-4055, doi: 10.5194/acp-6-3625-2006, 2006.

Boyd, A. A., Flaud, P. M., Daugey, N. and Lesclaux, R.: Rate constants for $RO_2 + HO_2$ reactions measured under a large excess of HO_2, J. Phys. Chem. A, 107, 818-821, doi: 10.1021/jp026581r, 2003.

Clark, J., Call, S. T., Austin, D. E. and Hansen, J. C.: Computational study of isoprene hydroxyalkyl peroxy radical-water complexes ($C_5H_8(OH)O_2$-H_2O), J. Phys. Chem. A, 114, 6534-6541, doi: 10.1021/jp102655g, 2010.

Clark, J., English, A. M., Hansen, J. C. and Francisco, J. S.: Computational study on the existence of organic peroxy radical-water complexes ($RO_2 \cdot H_2O$), J. Phys. Chem. A, 112, 1587-1595, doi: 10.1021/jp077266d, 2008.

Dovrou, E., Rivera-Rios, J. C., Bates, K. H. and Keutsch, F. N.: Sulfate formation via cloud processing from isoprene hydroxyl hydroperoxides (ISOPOOH), Environ. Sci. Technol., 53, 12476-12484, doi: 10.1021/acs.est.9b04645, 2019.

Gong, Y. W. and Chen, Z. M.: Quantification of the role of stabilized Criegee intermediates in the formation of aerosols in limonene ozonolysis, Atmos. Chem. Phys., 21, 813-829, doi: 10.5194/acp-21-813-2021, 2021.

Gong, Y. W., Chen, Z. M. and Li, H.: The oxidation regime and SOA composition in limonene ozonolysis: roles of different double bonds, radicals, and water, Atmos. Chem. Phys., 18, 15105-15123, doi: 10.5194/acp-18-15105-2018, 2018.

Huang, D., Chen, Z. M., Zhao, Y. and Liang, H.: Newly observed peroxides and the water effect on the

137 formation and removal of hydroxyalkyl hydroperoxides in the ozonolysis of isoprene, Atmos. Chem.
138 Phys., 13, 5671-5683, doi: 10.5194/acp-13-5671-2013, 2013.
139 Kircher, C. C. and Sander, S. P.: Kinetics and mechanism of HO_2 and DO_2 disproportionations, J. Phys.
140 Chem., 88, 2082-2091, doi: 10.1021/j150654a029, 1984.
141 Kumbhani, S. R., Cline, T. S., Killian, M. C., Clark, J. M., Keeton, W. J., Hansen, L. D., Shirts, R. B.,
142 Robichaud, D. J. and Hansen, J. C.: Water vapor enhancement of rates of peroxy radical reactions, Int. J.
143 Chem. Kinet., 47, 395-409, doi: 10.1002/kin.20917, 2015.
144 Lambe, A. T., Ahern, A. T., Williams, L. R., Slowik, J. G., Wong, J. P. S., Abbatt, J. P. D., Brune, W. H.,
145 Ng, N. L., Wright, J. P., Croasdale, D. R., Worsnop, D. R., Davidovits, P. and Onasch, T. B.:
146 Characterization of aerosol photooxidation flow reactors: heterogeneous oxidation, secondary organic
147 aerosol formation and cloud condensation nuclei activity measurements, Atmos. Meas. Tech., 4, 445-
148 461, doi: 10.5194/amt-4-445-2011, 2011.
149 Liu, Y. J., Herdlinger-Blatt, I., McKinney, K. A. and Martin, S. T.: Production of methyl vinyl ketone and
150 methacrolein via the hydroperoxyl pathway of isoprene oxidation, Atmos. Chem. Phys., 13, 5715-
151 5730, doi: 10.5194/acp-13-5715-2013, 2013.
152 Mao, J., Ren, X., Brune, W. H., Olson, J. R., Crawford, J. H., Fried, A., Huey, L. G., Cohen, R. C., Heikes,
153 B., Singh, H. B., Blake, D. R., Sachse, G. W., Diskin, G. S., Hall, S. R. and Shetter, R. E.: Airborne
154 measurement of OH reactivity during INTEX-B, Atmos. Chem. Phys., 9, 163-173, doi: 10.5194/acp-
155 9-163-2009, 2009.
156 McElroy, W. J. and Waygood, S. J.: Oxidation of formaldehyde by the hydroxyl radical in aqueous-
157 solution, CS. Faraday trans., 87, 1513-1521, doi: 10.1039/ft9918701513, 1991.
158 Monod, A., Chebbi, A., Durand-Jolibois, R. and Carlier, P.: Oxidation of methanol by hydroxyl radicals
159 in aqueous solution under simulated cloud droplet conditions, Atmos. Environ., 34, 5283-5294, doi:
160 10.1016/S1352-2310(00)00191-6, 2000.
161 Ruppert, L. and Heinz Becker, K.: A product study of the OH radical-initiated oxidation of isoprene:
162 formation of C_5-unsaturated diols, Atmos. Environ., 34, 1529-1542, doi:
163 https://doi.org/10.1016/S1352-2310(99)00408-2, 2000.
164 Sander, R.: Compilation of Henry's law constants (version 4.0) for water as solvent, Atmos. Chem. Phys.,
165 15, 4399-4981, doi: 10.5194/acp-15-4399-2015, 2015.
166 St Clair, J. M., Rivera-Rios, J. C., Crounse, J. D., Knap, H. C., Bates, K. H., Teng, A. P., Jorgensen, S.,
167 Kjaergaard, H. G., Keutsch, F. N. and Wennberg, P. O.: Kinetics and products of the reaction of the first-

generation isoprene hydroxy hydroperoxide (ISOPOOH) with OH, J. Phys. Chem. A, 120, 1441-1451, doi: 10.1021/acs.jpca.5b06532, 2016.

Winkelman, J. G. M., Ottens, M. and Beenackers, A. A. C. M.: The kinetics of the dehydration of methylene glycol, Chem. Eng. Sci., 55, 2065-2071, doi: 10.1016/S0009-2509(99)00498-4, 2000.

Winkelman, J. G. M., Voorwinde, O. K., Ottens, M., Beenackers, A. A. C. M. and Janssen, L. P. B. M.: Kinetics and chemical equilibrium of the hydration of formaldehyde, Chem. Eng. Sci., 57, 4067-4076, doi: 10.1016/S0009-2509(02)00358-5, 2002.

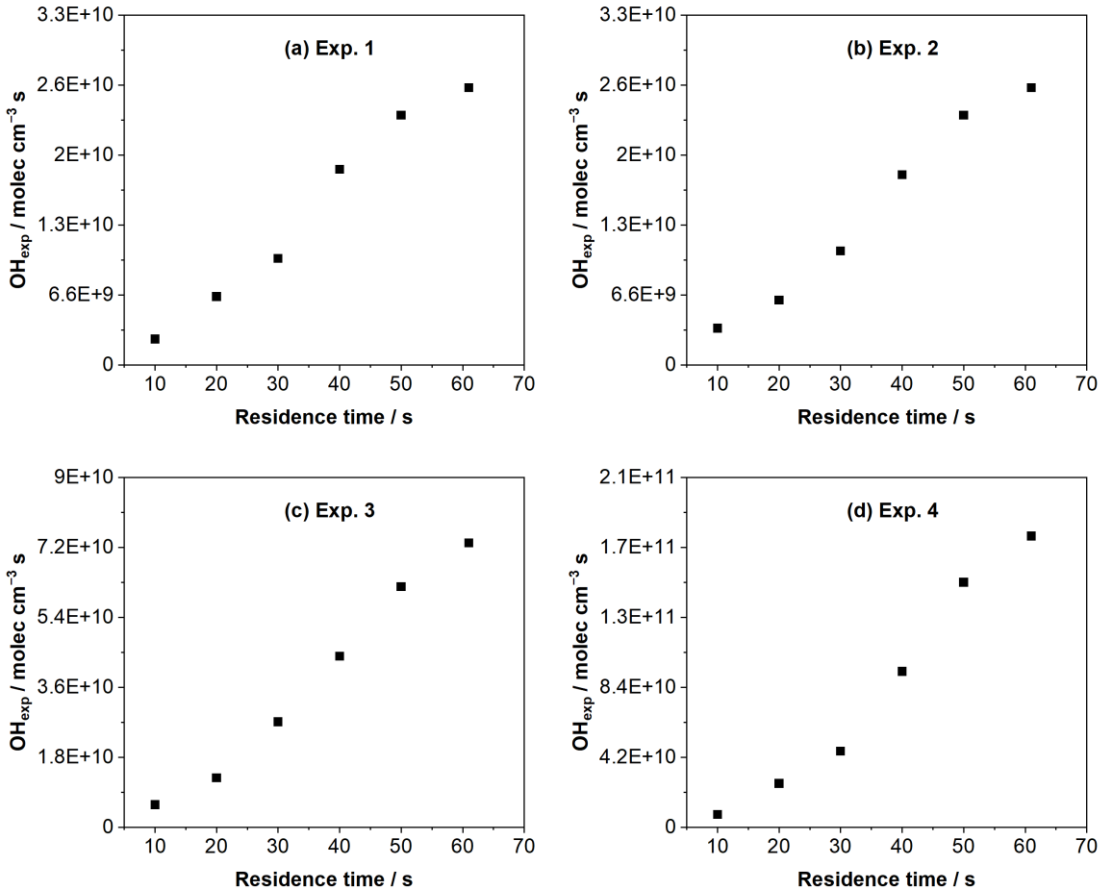

176

177 **Figure S1:** The evolution of OH_{exp} with residence time in Exp. 1−4 (a−d).

178

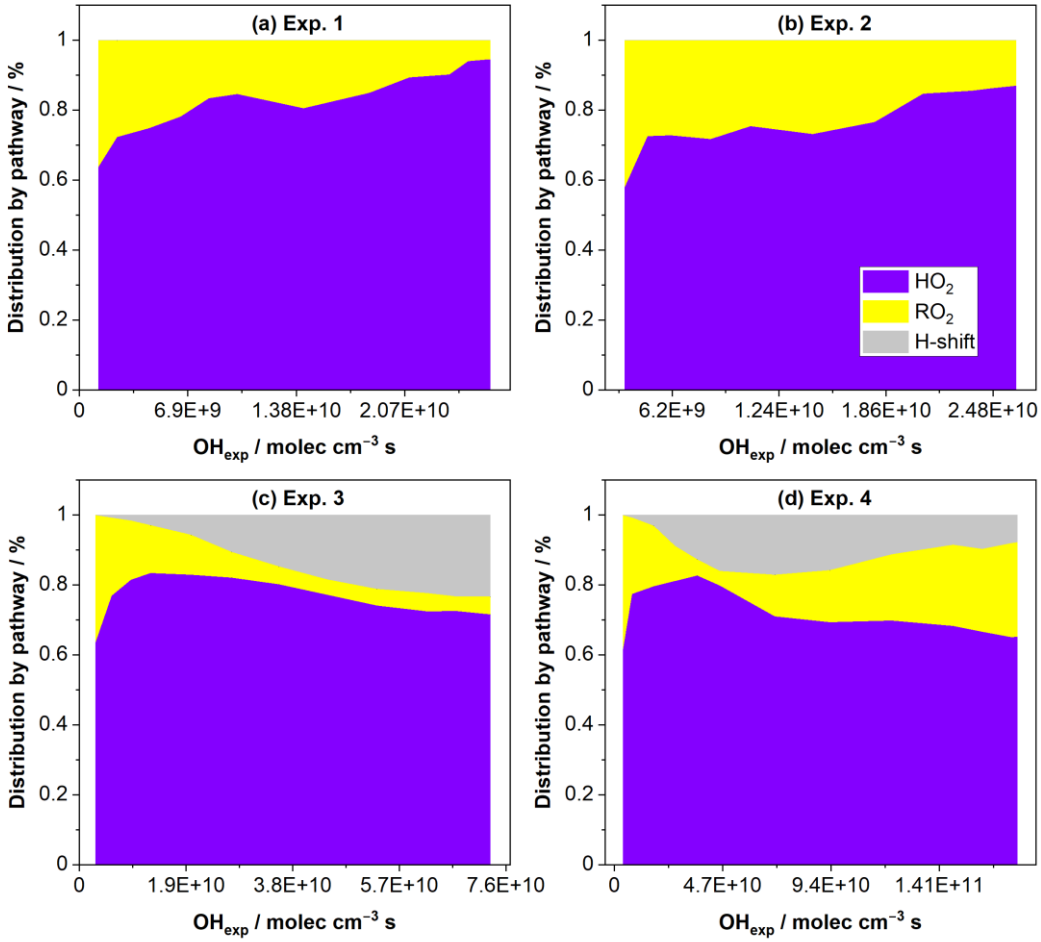

179

180 **Figure S2:** Distribution of reaction pathways of major RO_2 in the experiments. Major RO_2 refers to RO_2

181 species which consist of more than 90 % of total RO_2 concentrations. In (a) Exp. 1 and (b) Exp. 2 it refers

182 to β-ISOPOO, while in (c) Exp. 3 and (d) Exp. 4 refers to the assembly of a series of RO_2.

183

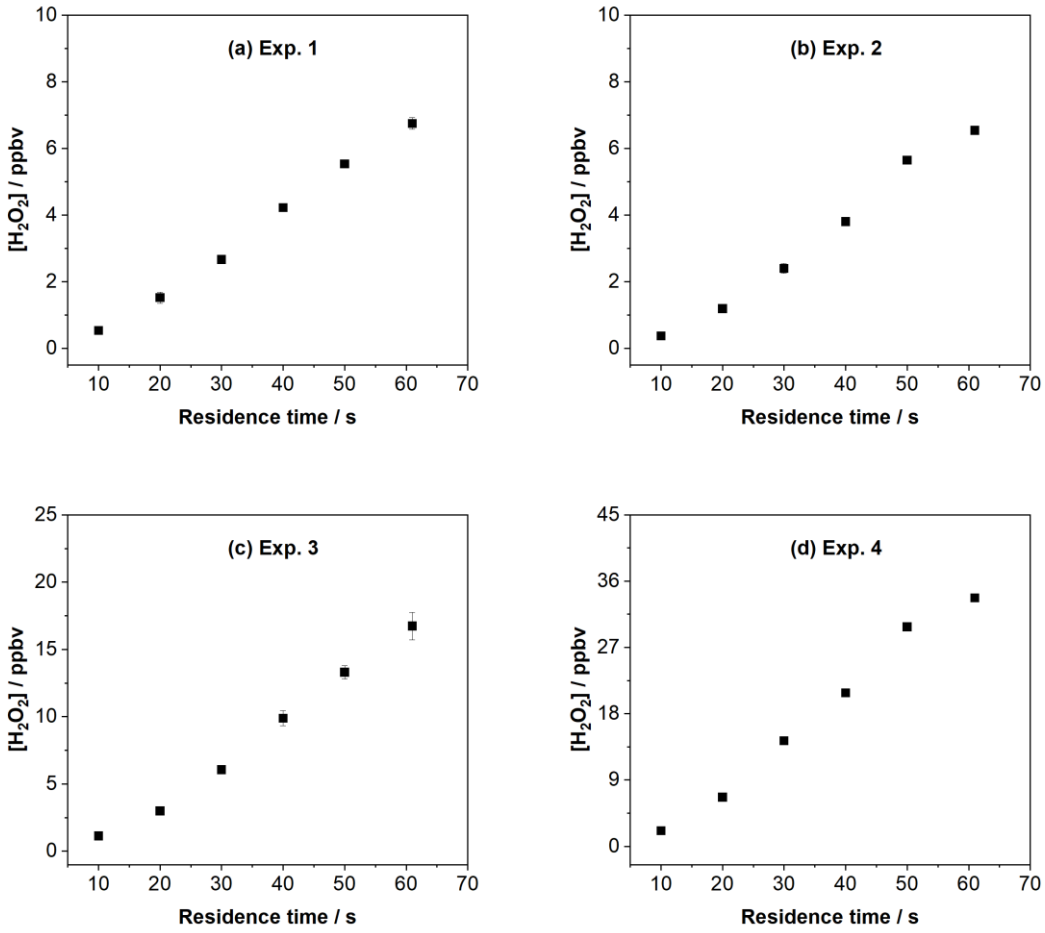

184

185 **Figure S3:** The observed evolution of H_2O_2 concentration in the experiments. Corrections have been
186 made to eliminate photolysis and wall loss of H_2O_2. The error bars represent ± standard deviation (± SD)
187 based on 6 measurements.

188

Table S1: Collection efficiencies for different species by the rinsing solution (5×10^{-3} M H_3PO_4 or ultrapure water) in the coiling tube at 277 K.

Species	Henry's law constant at 277 K/M atm^{-1}	Collection efficiency	References
FA	4.20E+04	99.5 %	Sander (2015)
AA	2.00E+04	98.9 %	
H2O2	5.80E+05	100.0 %	
HMHP	2.10E+07	100.0 %	
PFA	2.90E+03[a]	92.8 %	
MHP	1.20E+03	84.3 %	
PAA	3.20E+03	93.5 %	
1,2-ISOPOOH	7.00E+05[b]	100.0 %	Dovrou et al. (2019)
4,3-ISOPOOH	8.00E+04[b]	99.7 %	

Note: Henry's law constant at [a]278 K and [b]298 K.

Table S2: First-order wall loss rate constants ($k_{WALL,i}$) of the concerned products in the OFR.

Rate constants/s^{-1}	Species	RH = 30 %	RH = 80 %	References
Carbonyls	HCHO	1.70E-04	1.70E-04	Gong et al. (2018)
	HACE	3.02E-04	4.84E-04	
	GLY	3.93E-04	4.99E-04	
	MGL	4.86E-04	6.04E-04	
Peroxides	H2O2	2.97E-04	1.71E-03	Huang et al. (2013)
	PAA	1.71E-03	3.47E-03	
	HMHP	2.39E-03	4.83E-03	
	PFA	2.14E-04	4.01E-04	Gong et al. (2018)
Organic acids	AA	3.47E-04	3.47E-04	Gong and Chen (2021)

196 **Table S3:** First-order photolysis rate constants ($k_{PH,i}$) of the concerned products in the OFR.

Species	Photon flux at 254 nm/photons cm^{-2} s^{-1}	Absorption Cross-section/cm^2 $molec^{-1}$	Quantum Yield	Rate constants/s^{-1}
O3	1.57E+15	1.14E-17	1	1.80E-02
HCHO	1.57E+15	4.56E-21	0.8	5.74E-06
GLY	1.57E+15	1.6E-20	1	2.52E-05
MGL	1.57E+15	2.859E-20	1	4.50E-05
MACR	1.57E+15	1.78E-21	0.05	1.40E-07
MVK	1.57E+15	2.41E-21	0.69	2.62E-06
H2O2	1.57E+15	6.7E-20	1	1.06E-04
MHP	1.57E+15	3.23E-20	1	5.09E-05

197

198

Table S4: Second-order reaction rate constants of the concerned products with OH radicals at 298 K ($k_{PRO,i+OH}$). The reaction rate constants were abstracted from MCM v3.3.1 website (http://mcm.york.ac.uk/home.htt) except for that of HMHP and β-ISOPOOH, which were abstracted from Allen et al. (2018) and St Clair et al. (2016), separately.

	Species	Rate constants/cm^3 $molec^{-1}$ s^{-1}
Carbonyls	HCHO	8.49E-12
	HACE	4.45E-12
	GLY	9.70E-12
	MGL	1.31E-11
	MACR	2.68E-11
	MVK	2.01E-11
Peroxides	H2O2	1.70E-12
	PAA	3.70E-12
	HMHP	7.10E-12
	MHP	1.00E-11
	β-1,2-ISOPOOH	7.50E-11
	β-4,3-ISOPOOH	1.18E-10
Organic acids	AA	8.00E-13
	FA	4.50E-13

Table S5: Relative abundance of RO_2 (HO_2) water complexes ($R_{RO_2\ (HO_2)\cdot H_2O}$) at 298 K under 30 % and 80 % RH.

	β-1,2-ISOPOO	β-4,3-ISOPOO	β-HEP	HO_2
RH = 30 %	0.27 %	0.74 %	0.72 %	4.41 %
RH = 80 %	0.71 %	1.96 %	1.91 %	11.0 %

Table S6: Advanced mechanisms and kinetics of isoprene photooxidation to MCM v3.3.1 in the modeling in this study.

S/N	Reactions	RH dependent rate constants at 298 K[a]	Reference
1	β-1,2-ISOPOO + HO2 → β-1,2-ISOPOOH + O2	$(1.74 \times 10^{-11} + 1.49 \times 13.2 \times 10^{-44} \times e^{9538 / T} \times [H2O]) \times (1 - 4.25 \times 10^{-19} \times [H2O] + 7.18 \times 10^{-2})$	Boyd et al. (2003)[b] This study
2	β-4,3-ISOPOO + HO2 → β-4,3-ISOPOOH + O2	$(1.74 \times 10^{-11} + 2.47 \times 13.2 \times 10^{-44} \times e^{9538 / T} \times [H2O]) \times (1 - 4.25 \times 10^{-19} \times [H2O] + 7.18 \times 10^{-2})$	
3	β-1,2-ISOPOO + HO2 → MVK + O2 + OH + CH2OH	$(1.74 \times 10^{-11} + 1.49 \times 13.2 \times 10^{-44} \times e^{9538 / T} \times [H2O]) \times (4.25 \times 10^{-19} \times [H2O] + 7.18 \times 10^{-2})$	
4	β-4,3-ISOPOO + HO2 → MACR + O2 + OH + CH2OH	$(1.74 \times 10^{-11} + 2.47 \times 13.2 \times 10^{-44} \times e^{9538 / T} \times [H2O]) \times (4.25 \times 10^{-19} \times [H2O] + 7.18 \times 10^{-2})$	
5	CH2OH + O2 → HOCH2OO	1.03×10^{-11}	Grotheer et al. (1985)
6	CH2OH + CH2OH → C2H6O2	1.50×10^{-11}	Grotheer et al. (1985)
7	HOCH2OO → HCHO + HO2	1.53×10^{2}	Atkinson et al. (2006)
8	HOCH2OO + HO2 → HOCH2OOH + O2	$1.25 \times 10^{-11} \times 0.6$	
9	HOCH2OO + HO2 → HCOOH + H2O + O2	$1.25 \times 10^{-11} \times 0.4$	
10	HOCH2O2 + HOCH2O2 → HCOOH + CH2(OH)2 + O2	7.05×10^{-13}	
11	HOCH2O2 + HOCH2O2 → HOCH2O + HOCH2O + O2	5.54×10^{-12}	
12	HCHO + HO2 → HOCH2OO	7.90×10^{-14}	Jenkin et al. (2007)
13	CH2(OH)2 → HCHO + H2O	8.49×10^{-3}	Winkelman et al. (2000)
14	HCHO + H2O → CH2(OH)2	3.23×10^{-22}	Winkelman et al. (2002)
15	CH2(OH)2 + OH → CH(OH)2 + H2O	1.30×10^{-12}	Monod et al. (2000)
16	CH(OH)2 + O2 → HCOOH + HO2	5.81×10^{-12}	McElroy and Waygood (1991)
17	CH(OH)2 + CH(OH)2 → HCOOH + CH2(OH)2	2.33×10^{-12}	
18	CH(OH)2 + OH → HCOOH + H2O	5.81×10^{-15}	

[a] Units: $cm^3\ molec^{-1}\ s^{-1}$ for second-order reactions; s^{-1} for first-order reactions.

[b] The reaction rate constant of ISOPOO + HO_2 under dry conditions at 298 K, $1.74 \times 10^{-11}\ cm^3\ molec^{-1}\ s^{-1}$, was abstracted from Boyd et al. (2003).